ISSN 1330-3651 (Print), ISSN 1848-6339 (Online)
Received: 1 May 2025; Accepted: 22 September 2025

https://doi.org/10.17559/TV-20250501002635
Original scientific paper

Investigation of the Influence of Machining Parameters on Surface Roughness in Turning Operations and Machine Learning Application

Metin ZEYVELİ, Murat AYDIN*

Abstract: The performance of turning operations gradually depends on the machining parameters, and the most important parameter is the surface roughness quality. In this study, the effect of cutting speed and feed rate on the surface roughness in aluminium alloy 6082 (AA6082) machining, which is widely used in the automotive and aerospace sectors, was investigated experimentally and by machine learning prediction. In the experiments, three different cutting speeds (240, 300, and 360 m/min), three different feed rates (0.05, 0.1, and 0.15 mm/rev), and a constant depth of cut (0.5 mm) were used as machining parameters. In addition to machining parameters, the temperature, cutting forces, revolution, current, voltage, and power were measured. The workpiece was machined using uncoated cemented carbide cutting tools. Experimental results showed that the surface roughness increased with increasing feed rate and decreased with increasing cutting speed. The complete dataset was created from experiments by selecting measurements and machining parameters as inputs and surface roughness as output. Various machine learning models were implemented on this dataset, and different metric scores were used to select the best prediction performance of the machine learning models. Gradient Boosting (GB) exhibited superior prediction performance compared to the other tested algorithms, with an R^2 score of 0.98560. The GB model emerged as the most precise and accurate, characterized by the highest R^2 score, the lowest root mean squared error (0.12095), the lowest mean absolute error (0.09804), and the lowest mean squared error (0.01463) scores, respectively.

Keywords: CNC turning; machinability; machine learning; surface roughness

1 INTRODUCTION

The improvement of surface quality of machined parts is the primary objective in manufacturing, especially in turning operations. These processes, defined by material removal to achieve particular geometries, have various parameters to influence final surface quality, namely called surface roughness. Some studies have reported on surface quality and dimensional accuracy optimization. This study comprehensively evaluated the dimensional deviation, flank wear, and surface roughness during the dry turning of C45 steel [1]. A surface roughness of 0.297 μm was achieved in Inconel 625 alloy at a feed rate of 0.1 mm/rev and a corner radius of 0.8 mm [2]. The negative effects of vibration on surface quality were demonstrated through simulations [3]. A minimum roughness value of $Ra = 0.238$ μm was achieved in the machining of AISI steel with CVD-coated tools [4]. In addition, other studies focused on cutting tool performance and coating technologies for dry turning. A study reported that TiN-coated tools provided 30 times longer life than uncoated tools in the machining of AISI D2 steel and provided 90.5% cost savings [5]. Similarly, the performance of TiCN-based cermet and carbide cutting tools in the dry turning of tempered martensitic stainless steel was investigated, and the effects of the cutting speed, feed rate, and side cutting edge angle on the tool life were demonstrated [6]. PVD, CVD, and MT-CVD coating technologies have been compared for the machining of AISI 4140 steel [7]. Furthermore, the superiority of PVD-coated tools in the machining of Incoloy 825 has been demonstrated [8]. The optimum cutting speed for TiN+AlCrN-coated tungsten carbide and Al_2O_3 + TiC ceramic tools was 220 m/min [9].

The adaptation of artificial intelligence (AI) and machine learning (ML) into conventional manufacturing processes presents accurate and precise control over the production, resulting in improved efficiency and effectiveness [10]. Particularly in machining industries, the prediction of the final quality of the product by ML algorithms has become increasingly critical because machining parameters significantly affect the quality and strength of the final product [11]. There are also some studies in the literature on tool wear mechanisms and prediction. In this study, an artificial neural network-based tool wear prediction was developed in the machining of AISI 4140 hardened steel [12]. The effects of tool geometry on flank and crater wear in AISI 316L stainless steel were also modelled, and it was determined that large corner radii reduce wear [13]. Besides, there are studies in the literature on multi-criteria decision-making and optimization methods. Accordingly, the MAIRCA, RCA, EAMR, MARCOS, and TOPSIS methods were compared in the optimization of turning processes [14]. Another study used a genetic algorithm to obtain Pareto optimal solutions for AISI 1040 steel [15]. Similarly, the GRA and TOPSIS methods found the optimum value for dry turning at a cutting speed of 250 m/min and a feed rate of 0.10 mm/rev [16]. In another study, the Taguchi method achieved an estimation error of less than 8% for duplex stainless steel [17]. Moreover, in an approach for surface roughness prediction in CNC turning, BPNN achieved an RMS error of 2.26% in surface roughness prediction [18]. The ANN-genetic algorithm combination was validated for Inconel 601 with an error of less than 2% [19]. ANN achieved an estimation error of less than 3% in micro-turning operations [20]. Productivity increases have been demonstrated with TiCN-TiN coated tools for AISI 52100 steel [21]. A life cycle assessment was conducted for the environmentally friendly turning of Inconel 601 [22]. A self-propelled rotary lathe achieved 9.7% energy savings and 35.4% surface improvement [23]. In the study, a thermal and mechanical model was developed for AISI 1040 steel, and the effects of increasing temperature and forces in the absence of coolant were investigated [24].

This study focused on the effect of machining parameters on the surface roughness during the turning of AA6082 material and the prediction performances of machine learning algorithms. AA6082 serves high strength

and corrosion resistance, has high welding capability, and is particularly well-suited for the marine and automotive industries. There are limited studies focusing on the machining parameters of AA6082 during the turning operations. Likewise, surface roughness prediction and comparison of prediction performance of the different machine learning models using not only machining parameters but also temperature, cutting forces, revolution, and power features during the turning operation have not been studied yet.

2 MATERIAL AND METHODS

2.1 Experimental Setup

2.1.1 Workpiece Material

In this study, 6082 aluminium, which is a 6XXX series aluminium alloy, was used. AA6082-T6 is an aluminium alloy from the Al-Mg-Si series known for improving the mechanical properties with heat treatment [25]. This material is a heat-treatable aluminium-magnesium-silicon alloy known for its high strength, good corrosion resistance, and excellent weldability, used in the automobile industry, brake discs, brake housings, exterior panels, and many other parts; in heavy structures in railway wagons, truck guardrails, shipbuilding sector, bridges, military bridges, bicycle manufacturing, boilers, platforms, flanges, hydraulic systems and parts, mining equipment, pylons, towers; nuclear energy, ship masts and beams, scaffolding pipes and tubes, and rivets. This alloy offers strong resistance to atmospheric and marine corrosion. AA 6082 is preferred over similar alloys, such as 6061, owing to its slightly higher strength and versatility in harsh environments. The chemical composition and mechanical properties of AA 6082 are listed in Tab. 1 and Tab. 2 [26].

To be used in machinability tests, the workpiece with a diameter of Ø50 mm and a length of 185 mm was used. In order to eliminate the effects of one machine parameter group on another parameter group, the 5 × 5 mm grooves were machined prior to actual experiments.

Table 1 Chemical composition of AA6082-T6 (wt.%) [22]

Material	Fe	Si	Cu	Mn	Mg	Zn	Cr	Other	Al
AA6082-T6	0.5	0.7-1.3	0.1	0.4-1.0	0.6-1.2	0.2	0.15	0.15	Rest

Fig. 1 illustrates the stock geometry and the dimensions. As seen in Fig. 1, the length of the stock was split into six segments, which were labelled from A to F, with an equal length of 20 mm. Throughout the experiments, various machining parameter groups were performed on the different segments. Therefore, the surface roughness values for each machining parameter group were measured using the presented segments. After the successful turning with a constant 20 mm length, the machining experiment was immediately stopped.

Table 2 Mechanical properties of AA 6082 materials [26]

Yield Strength	Tensile Strength	Elongation	Hardness
N/mm²	N/mm²	%	HV
260-300	310-340	13	115

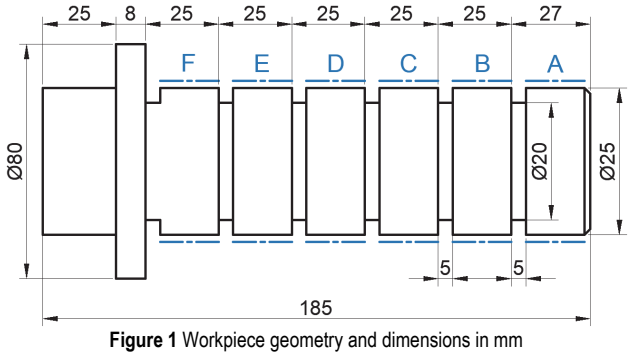

Figure 1 Workpiece geometry and dimensions in mm

2.1.2 Machine Tool, Cutting Tool, and Cutting Parameters

Machinability tests were carried out on a TaksanTMC 500 V CNC lathe. The power of the lathe is 10 kW, the spindle speed is 6000 rpm, the workpiece maximum length is 550 mm, the workpiece diameter is 400 mm, the precision is 0.001 mm, and the number of tool carriages is 12.

The cutting tool used was a Böhler brand commercial-quality uncoated cemented carbide cutting tool in the form of "TCGT 16T308-270G" and HB10-K10 grade (Fig. 2). The cutting tool was mechanically clamped in a tool holder of the STGCR2020K16 metric form, which was designed to have an engagement angle of 90°. The cutting tool and tool holder used in the experiments are shown in Fig. 2. The cutting tool specifications are *l*: 16.5, *s*: 3.97, *d*: 9.52, d_1: 4.4, *r*: 0.8 mm.

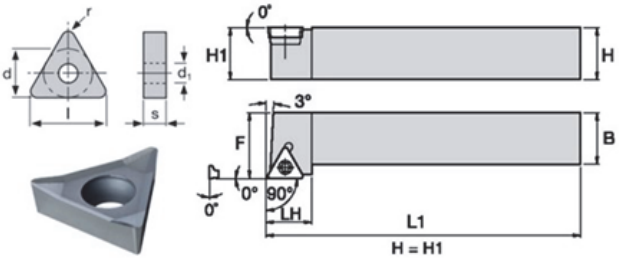

Figure 2 The view of the cutting tool and the tool holder

Regarding the machinability tests of the AA 6082 material, the cutting parameters given in Tab. 3 were used. The choice of cutting parameter values was based on the range of cutting tool manufacturer recommendations, and the values of cutting parameters were selected by considering the lower and upper limits of each parameter. For this purpose, three different cutting speeds of 240, 300, and 360 m/min were selected in the experiments. Three different values of 0.05, 0.1, and 0.15 mm/rev were selected for the feed rate. In the machinability experiments, the depth of cut was fixed at 0.5 mm because of the more accurate and precise analysis of cutting speed and feed rate effects on the surface roughness, and no coolant was used for better surface roughness measurements (Tab. 3).

Table 3 Cutting parameters of AA 6082 materials

Cutting Parameters	Unit	Level 1	Level 2	Level 3
Cutting Speed (V_c)	m/min	240	300	360
Feed Rate (f)	mm/rev	0.05	0.1	0.15
Depth of Cut (a)	mm	0.5		
Machining Condition	-	Dry		

The arithmetic roughness average (*Ra*) on turning surfaces was measured using a profilometer Marsurf PS1, with a cut off 0.8 mm, according to ISO/DIS 4287/1E. Surface roughness measurements were made by machining surface rotated 120° the three measurements and these measurements were obtained by taking the mean of the average surface roughness (*Ra*) values. In this study, a Kistler 9257 B piezoelectric-based dynamometer was employed to measure the cutting forces. The force values obtained from the dynamometer were conveyed to a Kistler Type 5070A multichannel charge amplifier and then to the computer via an RS-232C connecting cable. The cutting force data were obtained using the specialized software of the dynamometer Dynoware. The numerical values of the cutting force were determined by calculating the mean of the cutting force values in the effective cutting zone. Elevated temperature in the cutting zone and tool during the machining process was measured using an Optris CS LT non-contact pyrometer. The pyrometer was calibrated between 0 °C and 400 °C temperature range.

2.2 Machine Learning Process

2.2.1 Selection of Input Parameters

Pearson correlation coefficients are vital tools for quantitatively assessing the linear relationships among multiple features and outputs for data analysis and decision-making [27]. Pairwise Pearson's correlation coefficients were calculated between the features and output in the present dataset. Thus, a 10 × 10 symmetric matrix was obtained with coefficients ranging from –1 to 1, as seen in Fig. 3.

Figure 3 Pearson's correlation matrix

The values of the coefficients are color-coded, and the colour scale is shown on the right side of the Fig. 3. According to the colour scale, negative values are represented in skin colour and light pink, whereas positive values are shown in darker colours.

2.2.2 Machine Learning Process

Supervised ML algorithms that have labelled inputs and outputs have promising potential to deal with various predictive engineering tasks by revealing intrinsic patterns and extracting significant insights from intricate datasets, recognizing linear and non-linear relationships between multiple features and outputs [28]. In the present study, 14 various ML algorithms were selected from the literature, which were widely used in regression studies. The performed algorithms were Multiple Linear Regression (MLR), Multi-Layer Perceptron (MLPR), Decision Tree (DT), Random Forest (RF), AdaBoost (AB), Bagging Regression (BR), Extra Trees (ET), Gradient Boosting (GB), Support Vector Machine (SVM), Linear SVM (LSVM), k-Nearest Neighbors (k-NN), XGBoost (XGB), XGBoost Random Forest (XGBRF), and Catboost (CatB). The schematic workflow of the ML process is given in Fig. 4. After the measurement of data from the experiments, the dataset was created and imported into the computer environment. The example set of used dataset is shown in Tab. 4. The ML process was performed using Python 3.9 software because of its easy and flexible syntax structure, and several classes were installed as NumPy 1.26.4, Pandas 2.2.3, and Scikit-learn 2.2.3. The data cleaning process was achieved initially by removing rows with zero values and highly noisy signals. After this step, feature engineering was performed by selecting the features and outputs and removing the set and reference columns. When data preprocessing was completed, the entire dataset was split into 80% for the training set and 20% for the test set because this ratio is reported as a suitable splitting ratio in terms of having enough data for training and test sets [29]. When the dataset was split, standardization, which is one of the feature scaling methods, was applied to the dataset to ensure that the features and outputs were on the same scale. The literature states that the standardization feature is a useful feature scaling technique in terms of improving model performance and reducing the impact of outliers [30]. Before training the model, to ensure the reliability and robustness of ML algorithms for the present dataset, the k-fold process was applied to the dataset by repeating 10-fold cross-validation 100 times among the algorithms and averaging the evaluation scores to obtain sufficient accuracy and prediction performance. This approach allows the validation of the algorithms in terms of gradually reducing overfitting and providing highly accurate and precise predictions of model performance on unseen data [31]. The evaluation metrics for the k-fold and final performance of the ML algorithms were selected as the coefficients of determination (R^2, seen in Eq. (1)), root mean squared error (*RMSE*), as shown in Eq. (2)), mean absolute error (*MAE*), as shown in Eq. (3)), and the mean squared error (*MSE*, as shown in Eq. (4)) because these metrics were stated as essential metrics for assessing the accuracy and reliability of ML algorithms throughout various applications [32]. To conduct initial evaluations of ML models, the *MAE* scores of k-fold results were taken into account due to the *MAE* scores showing alterations between the measured and predicted values because they exhibit decreased sensitivity to particular errors. Therefore, the threshold for the *MAE* score was set at 0.20 since this value was reported as satisfactory for particular applications [33].

$$R^2 = 1 - \frac{\sum_{i=1}^{n}(x_i - y_i)^2}{\sum_{i=1}^{n}(\bar{y} - y_i)^2} \quad (1)$$

Table 4 Example set of created dataset from experiements

Inputs									Output
Cutting Speed	Feed Rate	Temperature	Rpm	Tangential Force	Feed Force	Current	Voltage	Power	Surface Roughness
m/min	mm/rev	°C	rev/min	N	N	A	V	Watt	µm
240	0.05	39.79	1528	9.12	3.13	3.20	91.29	292.11	2.551
240	0.10	40.53	1528	15.95	5.66	3.53	97.30	342.99	1.331
240	0.15	41.31	1528	21.20	6.10	4.09	90.88	371.96	1.870
300	0.05	40.97	1910	7.36	2.42	2.76	112.30	309.63	1.338
300	0.10	41.53	1910	13.40	4.15	3.24	108.54	351.86	1.439
300	0.15	41.94	1910	17.13	4.56	3.45	113.97	393.17	1.538
360	0.05	41.89	2300	5.92	1.39	2.83	121.88	345.47	0.965
360	0.10	42.85	2300	9.92	1.96	3.39	120.88	409.23	1.825
360	0.15	43.37	2300	14.26	2.42	3.81	117.05	446.01	2.847

$$RMSE = \sqrt{\frac{1}{n}\sum_{i=1}^{n}(x_i - y_i)^2} \quad (2)$$

$$MAE = \frac{1}{n}\sum_{i=1}^{n}|x_i - y_i| \quad (3)$$

$$MSE = \frac{1}{n}\sum_{i=1}^{n}(x_i - y_i)^2 \quad (4)$$

3 RESULTS AND DISCUSSION

3.1 Turning Results

The parameters listed in Tab. 3 were used in the experimental procedures. While conducting experimental studies using the parameters given in this table, values such as tangential force, feed force, temperature at the tool-chip interface, and the current and voltage drawn by the machine during the cutting process were also measured and recorded. These data were analysed to determine the effects of the measured parameters on the machining process.

Fig. 5a illustrates the graphs of variables such as the measured forces during the cutting process and the temperature at the tool-chip interface over time for each experimental parameter. Due to the millisecond-level data recording in these graphs, the resulting data exhibit high amplitude, complicating analysis and evaluation. Consequently, similar to the averaging of three repeated surface roughness measurements, the averages of these data were computed and assessed for each cutting parameter.

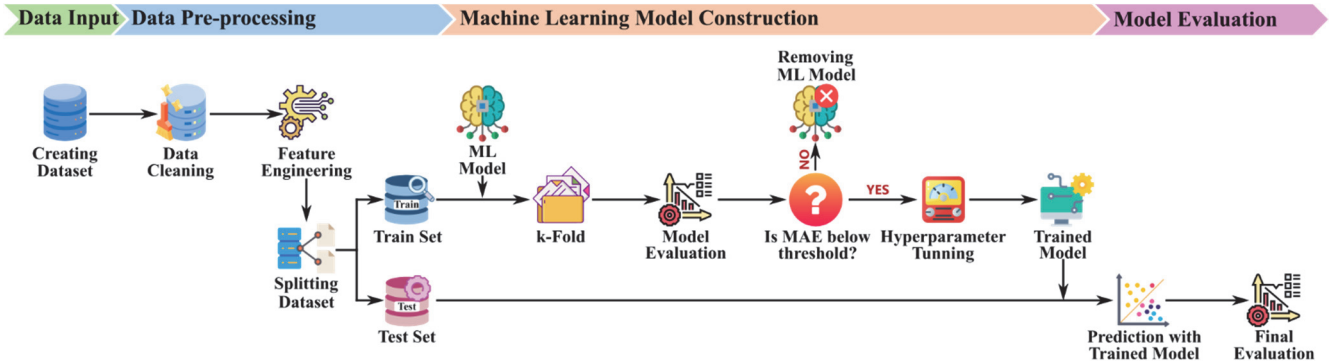

Figure 4 Schematic workflow of the ML process

The surface roughness graph according to the cutting speed and feed rate is shown in Fig. 5b. The surface roughness values generally increased at all cutting speeds with the increase in feed rate (from 0.05 to 0.15 mm/rev). This indicates that the feed rate has a significant impact on surface quality. At a cutting speed of 240 m/min (blue columns), the surface roughness is relatively high at the lowest feed rate (0.05 mm/rev) (~2.5 µm). However, as the feed rate increases, the roughness first decreases (to ~1.3 µm at 0.10 mm/rev), then increases again (to ~1.8 µm at 0.15 mm/rev). At a cutting speed of 360 m/min, the lowest roughness value (~0.9 µm) was obtained at the lowest feed rate (0.05 mm/rev). As the feed rate increases, the roughness significantly increases (approximately 2.8 µm at 0.15 mm/rev). This situation is thought to be due to the sharper chip breaking mechanism that occurs at high cutting speeds and the softer material forming a smoother surface owing to the heat effect. Similar results were noted in the study conducted by Garcia et al. [34] compared to the literature.

The graph of tangential and axial forces generated during the turning process is shown in Fig. 3c and Fig. 3d. In the graph, it was observed that the forces increased with an increase in the feed rate but decreased with an increase in the cutting speed. This situation causes a decrease in cutting speeds owing to the softening of the material by heat at high cutting speeds, while the increase in the feed rate leads to an increase in the amount of chips removed, resulting in higher forces. Özlü [35] obtained similar results in his study.

In the experimental study, the temperature at the tool-chip interface during the cutting process was measured. According to the processing parameters, this temperature change is shown in Fig. 5e. As seen in this graph, the temperature increases at all cutting speeds with an increase in the feed rate. This situation has caused an increase in temperature owing to the deformation occurring during the cutting process, as the volume of chips removed increases with the increase in feed rate. Similarly, the change in cutting speed caused an increase in temperature. However,

as seen in Fig. 5e, we can say that the change in cutting speed has a greater effect on temperature. The reason for this situation can be expressed as it is known from the literature that the increase in temperature reduces shear strength, and the increase in contact length increases shear force [36].

In the machining process, the power consumed as a function of the feed rate-cutting speed is shown in Fig. 5f. At a constant cutting speed, the power consumed increased linearly as the feed rate increased. This situation means that at high feed rates, the amount of chips removed by the cutting tool per unit time increases, which results in more mechanical work and consequently higher power consumption; this is also supported by the literature [37].

At a constant feed rate, as the cutting speed increased, the power consumed also increased. This situation is discussed in the article by [38]. As the cutting speed increased, the amount of material processed per unit time increased, and higher temperatures were generated in the cutting zone. This also increases the energy consumption owing to friction and deformation.

The highest power consumption (approximately 450 W), the highest cutting speed (360 m/min), and the highest feed rate (0.15 mm/rev) were observed. The lowest power consumption (approximately 290 W), the lowest cutting speed (240 m/min), and the lowest feed rate (0.05 mm/rev) were observed. The results obtained here are consistent with findings from the literature, specifically studies by [39, 40]. Again, when the slopes of the curves were examined, it was observed that, as the cutting speed increased, the effect of the feed rate on power consumption became more pronounced. In this case, it shows similarity with the findings in the literature. interaction can be explained by the analyses of the relationships between processing parameters in the study by [41].

3.2 Performance Evaluation of Machine Learning Models

In the present study, pre-performance evaluations of the ML models were interpreted in terms of the MAE scores of the k-fold process, given in Tab. 5. ML algorithms that produced MAE scores below the threshold through the k-fold process were eliminated for further prediction. Before the final prediction, hyperparameter tuning was established by a randomized search cross-validation technique to decrease the calculation time and prevent computer performance from being constant because this technique was reported to be particularly advantageous for providing efficient search processes and leading to better model performance [42]. For the final prediction, tuned ML algorithms were performed and compared with the test set in terms of evaluation metrics for the current dataset. The tested models, with the exception of the MLR and LSVM models, produced MAE scores below the threshold of 0.20, which indicated higher prediction performance, as seen in Tab. 5.

Table 5 *MAE* scores of ML algorithms for the k-fold process

	MLR	MLPR	DT	RF	AB	BR	ET
MAE	0.56502	0.10457	0.14294	0.12906	0.15922	0.13066	0.14198
	GB	**SVM**	**LSVM**	**k-NN**	**XGB**	**XGBRF**	**CatB**
MAE	0.10341	0.10433	0.49496	0.10548	0.13372	0.10006	0.11283

Tab. 6 compares the final prediction metric scores of the present ML algorithms in the current study. Based on the evaluation of metric scores, it is seen that the GB outperforms the other algorithms in terms of the R^2 score of 0.98560, the *MAE* score of 0.09804, and the MSE score of 0.01463, respectively. The GB algorithm can provide superior efficiency in minimizing the error rate between measured and predicted values, exhibiting improved prediction accuracy than the other algorithms because it produces the highest R^2 score and the lowest *RMSE*, *MAE*, and *MSE* scores. In addition, as shown in Fig. 6a, the data points of the GB algorithm are ideally close to the regressed diagonal line and have fewer outliers with acceptable distances from the line. It is possible to conclude that the GB algorithm has a robust goodness of fit, with most predicted surface roughness outputs closely aligning with the measured surface roughness values for the present dataset.

When considering the R^2 and *MAE* scores, it can be seen that the XGBRF with an R^2 score of 0.98544 and *MAE* score of 0.10001 is ranked as the second-best prediction performance, and k-NN with an R^2 score of 0.98503 and *MAE* score of 0.10629 is the third-best prediction model. Although the GB algorithm gives the best R^2 and *MAE* scores, as it exhibits better prediction capability in the present study, it may be seen that the XGBRF and k-NN algorithms come in very close proximity in terms of R^2 and *MAE* scores. It can also be observed that negligible differences of approximately 0.00016 and 0.00057 exist between the highest R^2 scores of the GB-XGBRF and GB-k-NN algorithms, respectively, making those algorithms comparable, as they surpass the performance of the other evaluated algorithms, as seen in Fig. 6b and Fig. 6c.

In terms of evaluation for tree-based ML algorithms, it is seen that DT, RF, AB, BR, ET, GB, XGB, XGBRF, and CatB algorithms gave a high R^2 score over 0.90, where it was reported that R^2 value of 0.8 or higher signified a strong indicator reliability and robustness of the model and an *MAE* of less than 15% may still be acceptable [43, 44]. Therefore, it is possible to mention that tree-based algorithms other than GB and XGBRF can considerably give acceptable performances in terms of the R^2 score, which varies from 0.95658 to 0.98560 for the present study. This can also be seen in the alignment of the predicted data points on the regressed diagonal line, as seen from Fig. 6d to Fig. 6j. Zhao stated that the higher prediction capability of tree-based algorithms is that employing an ensemble method by averaging predictions from multiple trees has increased the robustness and accuracy of modelling varied datasets [45]. Amin et al. stated that R^2 over 80% highlights the dealing capability of tree-based algorithms more effectively with high-dimensional and non-linear relationships between features and outputs than other algorithms by eliminating overfitting and variance, increasing prediction accuracy by capturing local patterns, detecting feature interactions automatically, and handling missing values and outliers [46].

From Tab. 5, it is also observed that the k-NN algorithm is among the top three algorithms with the best prediction performance in terms of higher R^2 and lower *MAE* scores than other tree-based algorithms, with the exception of GB and XGBRF. In addition, it is shown that the data points of the k-NN are well aligned to the regressed diagonal line, as shown in Fig. 6c.

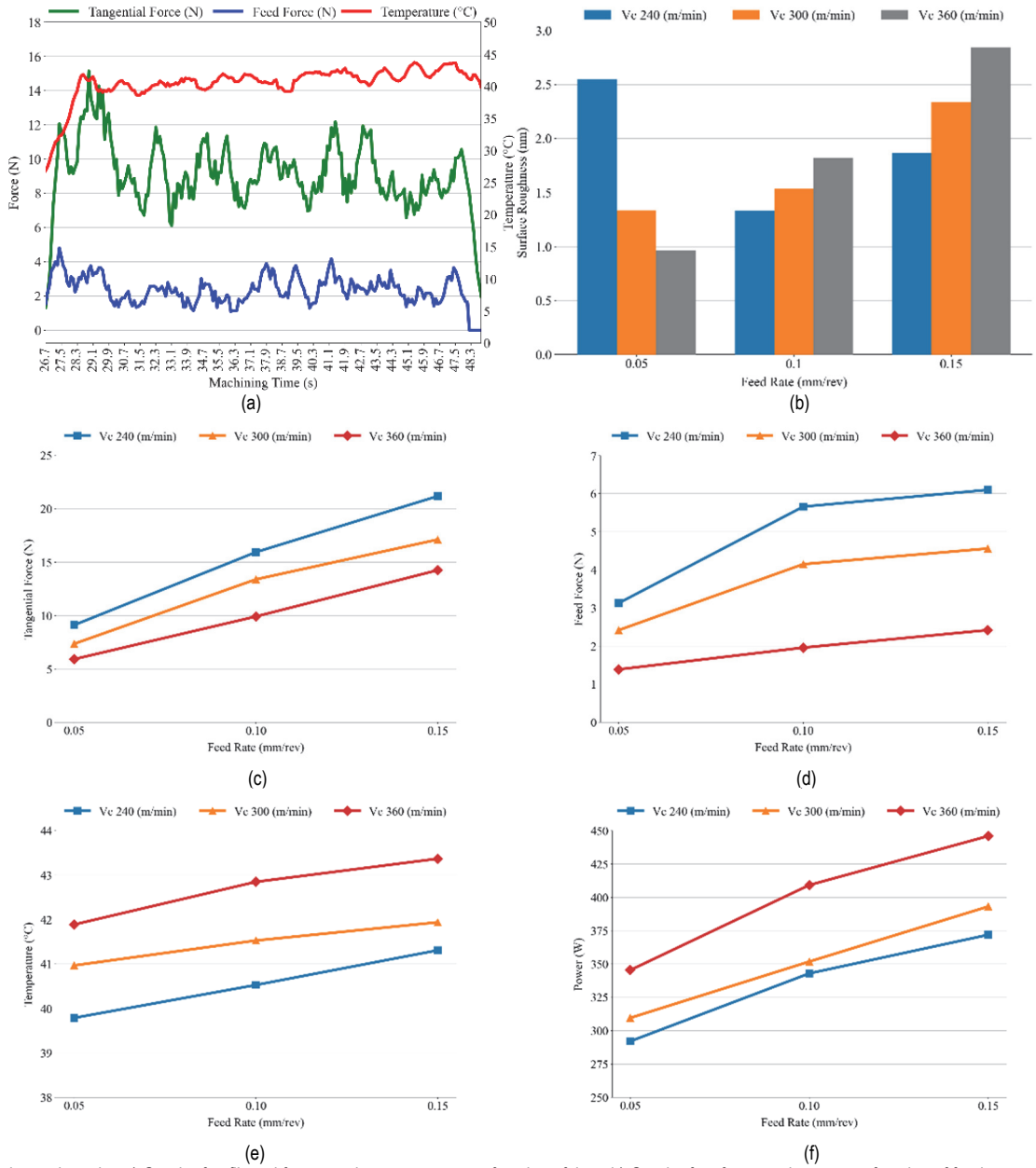

Figure 5 Experimental results: a) Graph of unfiltered forces and temperature as a function of time; b) Graph of surface roughness as a function of feed rate and cutting speed; c) Variation in tangential force with respect to feed rate and cutting speed; d) Variation in axial force with respect to feed rate and cutting speed; e) Variation in temperature with respect to feed rate and cutting speed; f) Variation in power with respect to feed rate and cutting speed

Table 6 Comparison of evaluation metric scores of ML models for final prediction

	MLR	MLPR	DT	RF	AB	BR	ET	GB	SVM	LSVM	k-NN	XGB	XGBRF	CatB
R^2	0.46727	0.97911	0.97351	0.97752	0.95658	0.96626	0.97355	**0.98560**	0.98456	0.35208	0.98503	0.97594	0.98544	0.98260
RMSE	0.73572	0.14570	0.16407	0.15112	0.21004	0.18516	0.16394	**0.12095**	0.12526	0.81137	0.12335	0.15635	0.12163	0.13298
MAE	0.58185	0.11022	0.14253	0.12985	0.17905	0.13939	0.14240	**0.09804**	0.10241	0.50960	0.10629	0.13514	0.10001	0.11368
MSE	0.54128	0.02123	0.02692	0.02284	0.04412	0.03428	0.02688	**0.01463**	0.01569	0.65832	0.01521	0.02444	0.01480	0.01768

Note: Best scores are described in bold.

Therefore, it can be assumed that the standardization process caused this phenomenon by scaling the features to have a mean of zero and a standard deviation of one, decreasing all data points to the same scale. It is reported that all features contribute uniformly to the distance computations by the standardization process; hence, the capability of the algorithm to identify nearest neighbours is increased gradually [47]. Furthermore, the non-parametric nature of k-NN may lead to flexibility in the underlying data distribution without imposing strict assumptions, potentially resulting in improved generalization of new data [48].

Moreover, the SVM and MLPR algorithms performed well regarding R^2 and *MAE* scores of 0.98456 and 0.10241 for the SVM algorithm, and 0.97911 and 0.11022 for the MLPR algorithm, respectively, as shown in Tab. 5. When comparing the evaluation metrics of SVM and MLPR with the GB algorithm metrics, it is observed that the R^2 score differences are approximately 0.00104 and 0.00649, and the *MAE* score differences are approximately 0.00437 and 0.01218, respectively. The data point distributions of SVM and MLPR close to the diagonal regressed line and fewer outliers make those algorithms still acceptable for predicting surface roughness in the present study, as seen

in Fig. 7a for SVM and Fig. 7c for MLPR. Choubey et al. [49] pointed out that the nature of SVM is to identify an optimal hyperplane to maximize the margin between data points and minimize errors. On the other hand, Ahmed [50] mentioned that the working principle of MLPR by building multiple layers of interconnected neurons to handle complex non-linear relationships and patterns. Thus, this makes both algorithms essential tools for dealing with regression problems.

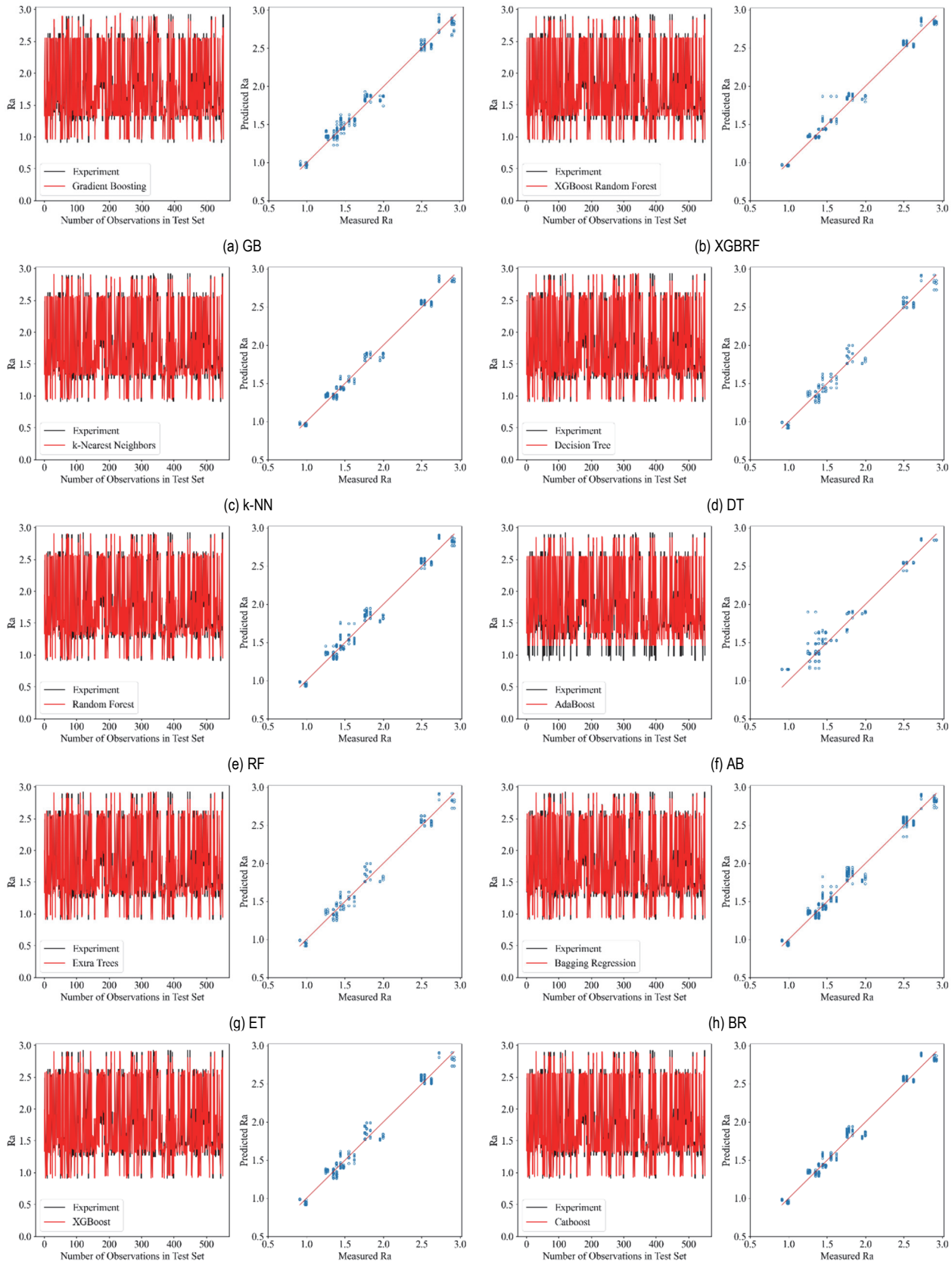

Figure 6 Surface roughness predictions using the GB, XGBRF, k-NN, DT, RF, AB, ET, BR, XGB, and CatB algorithms

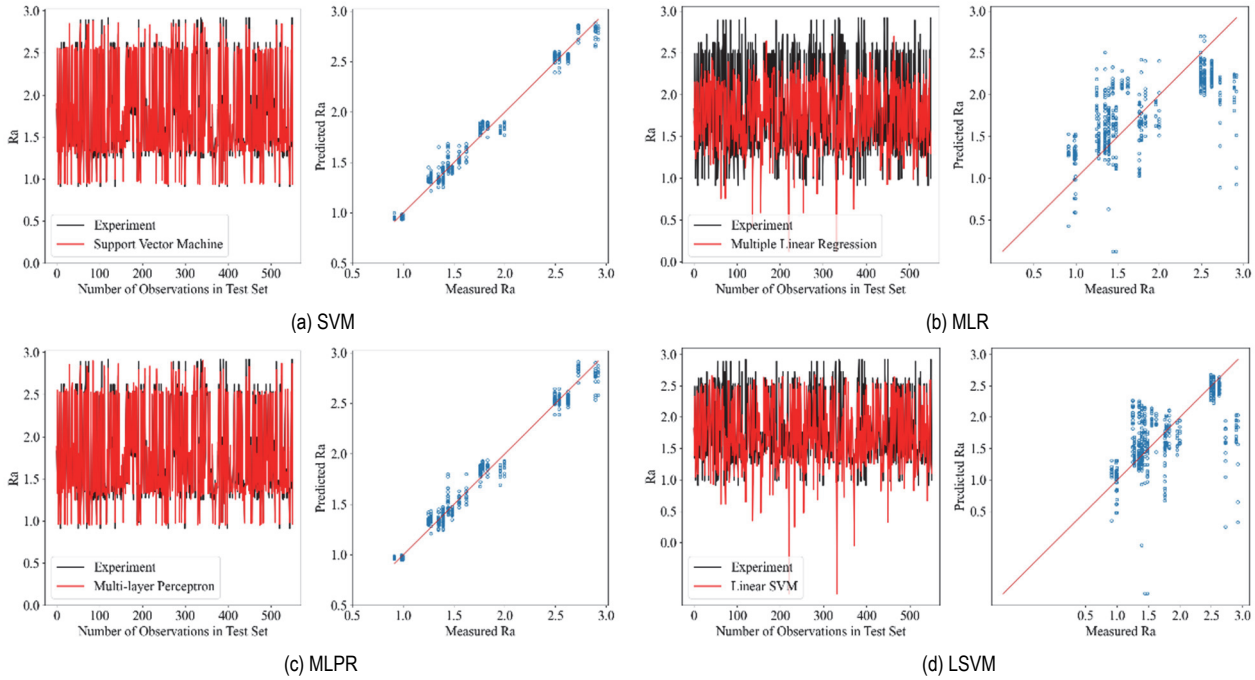

Figure 7 Surface roughness predictions using the SVM, MLR, MLPR, and LSVM algorithms

In addition, there is a noticeable contrast in terms of evaluation metrics between MLR, LSVM, and the other tested algorithms. Based on Tab. 5, MLR and LSVM algorithms perform similarly, and it can be deduced that the performances of MLR and LSVM algorithms are significantly poor when compared to the other algorithms owing to R^2 scores of 0.46727 and 0.35208, respectively. In addition to the lower R^2 scores of the MLR and LSVM algorithms, higher *MAE* scores of 0.58185 and 0.50960 reflect the poorest prediction performance of those algorithms because the number of outliers is higher than other tested algorithms in the present study, as seen in Fig. 7b and Fig. 7d. Studies have shown that MLR [51] and LSVM [52] algorithms are based on the assumption of a linear relationship between the features and outputs, and this approach prevents them from capturing nonlinearity and complex feature interactions in the dataset.

Several studies have shown that machine-learning techniques have the flexibility and capability to be integrated into various machining processes, especially in terms of prediction of cutting forces [53], tool life estimation [54] and prediction of surface roughness [55]. In the present study, tree-based ML algorithms, especially GB and XGBRF, have been shown to produce better surface roughness prediction performances than the other tested algorithms regarding the highest R^2 and lowest *MAE* and *MSE* evaluation metrics. Patel [56] and Nguyen [57] demonstrated the effectiveness and simplicity of the GB algorithm over other tested algorithms by achieving a satisfactory R^2 score of 0.9206 for surface roughness prediction. Moreover, Gadagi [58] and Prasad [59] reported that tree-based algorithms, such as the XGB and GBR models, have higher accuracy in estimating the surface roughness in terms of dealing with the capability of missing values and generalization properties owing to the built-in regularization process by means of improved optimization techniques and capturing complex intrinsic patterns. In addition, among all ML algorithms, tree-based and ensemble ML algorithms have been especially preferred for regression tasks. In the literature, it is reported that tree-based and ensemble ML algorithms have higher prediction capabilities with lower error rates because they can easily handle complex and high-dimensional datasets and fit nonlinear relationships [60].

4 CONCLUSION

The study presents the relationship between machining parameters and surface roughness from turning AA 6082 material experimentally and compares the performance of various machine learning models in predicting surface roughness. In the experimental methodology, three cutting speeds and three feed rates were used under a constant depth of cut. Throughout the turning operation, temperature, cutting forces, current, voltage, and power data were measured. The turning experiments and machine learning applications have provided valuable insights into the machining parameters on the surface roughness. The key findings can be summarized as follows:

- The most significant machining parameters affecting the surface roughness were determined to be cutting speed and feed rate. The lowest surface roughness of 0.965 µm was obtained at a cutting speed of 360 m/min and a feed rate of 0.05 mm/rev, while the highest surface roughness of 2.847 µm was obtained with a feed rate of 0.15 mm/rev.
- Regarding the tool-chip interface temperature, tangential force (12%) and cutting speed (5.7%) were identified as the most significant parameters.
- The most effective machining parameters on the power consumption were the feed rate (57%) and the cutting speed/revolution rate (37%), showing the importance of those in optimizing the energy efficiency of the turning process.
- In terms of surface roughness prediction, the Gradient Boosting (GB) model outperformed others, achieving an R^2 score of 0.98560. This result underscores its

effectiveness in accurately estimating surface roughness during the turning of aluminium alloy.

5 REFERENCES

[1] Milosevic, A., Simunovic, G., Kanovic, Z., Simunovic, K., Santosi, Z., Sokac, M., & Vukelic, D. (2024). Comprehensive evaluation of dimensional deviation, flank wear, surface roughness and material removal rate in dry turning of C45 steel. *Facta Universitatis, Series: Mechanical Engineering*, 547. https://doi.org/10.22190/FUME240403024M

[2] Vukelic, D., Milosevic, A., Ivanov, V., Kocovic, V., Santosi, Z., Sokac, M., & Simunovic, G. (2024). Modelling and optimization of dimensional accuracy and surface roughness in dry turning of Inconel 625 alloy. *Advances in Production Engineering & Management*, *19*(3), 371-385. https://doi.org/10.14743/apem2024.3.513

[3] Kang, W. T., Derani, M. N., & Ratnam, M. M. (2020). Effect of vibration on surface roughness in finish rurning: Simulation study. *International Journal of Simulation Modelling*, *19*(4), 595-606. https://doi.org/10.2507/IJSIMM19-4-531

[4] Vukelic, D., Prica, M., Ivanov, V., Jovicic, G., Budak, I., & Luzanin, O. (2022). Optimization of surface roughness based on turning parameters and insert geometry. *International Journal of Simulation Modelling*, *21*(3), 417-428. https://doi.org/10.2507/IJSIMM21-3-607

[5] Sahoo, A. K. & Sahoo, B. (2013). A comparative study on performance of multilayer coated and uncoated carbide inserts when turning AISI D2 steel under dry environment. *Measurement*, *46*(8), 2695-2704. https://doi.org/10.1016/j.measurement.2013.04.024

[6] Noordin, M. Y., Venkatesh, V. C., & Sharif, S. (2007). Dry turning of tempered martensitic stainless tool steel using coated cermet and coated carbide tools. *Journal of Materials Processing Technology*, *185*(1-3), 83-90. https://doi.org/10.1016/j.jmatprotec.2006.03.137

[7] Hamadi, B., Yallese, M. A., Boulanouar, L., Hammoudi, A., & Nouioua, M. (2022). Evaluation of the cutting performance of PVD, CVD and MTCVD carbide inserts in dry turning of AISI 4140 steel using RSM-based NAMDE optimization. *Journal of the Brazilian Society of Mechanical Sciences and Engineering*, *44*(8), 342. https://doi.org/10.1007/s40430-022-03633-5

[8] Thakur, A., Gangopadhyay, S., Maity, K. P., & Sahoo, S. K. (2016). Evaluation on effectiveness of CVD and PVD coated tools during dry machining of Incoloy 825. *Tribology Transactions*, *59*(6), 1048-1058. https://doi.org/10.1080/10402004.2015.1131350

[9] Saikaew, C., Paengchit, P., & Wisitsoraat, A. (2020). Machining performances of TiN+AlCrN coated WC and Al2O3+TiC inserts for turning of AISI 4140 steel under dry condition. *Journal of Manufacturing Processes*, *50*, 412-420. https://doi.org/10.1016/j.jmapro.2019.12.057

[10] Bappy, M. A. (2024). Exploring the integration of informed machine learning in engineering applications: A comprehensive review. *American Journal of Science and Learning for Development*, *3*(2), 11-21. https://doi.org/10.51699/ajsld.v3i2.3459

[11] du Preez, A. & Oosthuizen, G. A. (2019). Machine learning in cutting processes as enabler for smart sustainable manufacturing. *Procedia Manufacturing*, *33*, 810-817. https://doi.org/10.1016/j.promfg.2019.04.102

[12] Rajeev, D., Dinakaran, D., & Singh, S. C. E. (2017). Artificial neural network based tool wear estimation on dry hard turning processes of AISI4140 steel using coated carbide tool. *Bulletin of the Polish Academy of Sciences Technical Sciences*, *65*(4), 553-559. https://doi.org/10.1515/bpasts-2017-0060

[13] Vukelic, D., Simunovic, K., Ivanov, V., Sokac, M., Kocovic, V., Santosi, Z., & Simunovic, G. (2024). Modelling of flank and crater wear during dry turning of AISI 316L stainless steel as a function of tool geometry using the response surface design. *Tehnicki Vjesnik - Technical Gazette*, *31*(4). https://doi.org/10.17559/TV-20231226001235

[14] Trung, D. D. & Thinh, H. X. (2021). A multi-criteria decision-making in turning process using the MAIRCA, EAMR, MARCOS and TOPSIS methods: A comparative study. *Advances in Production Engineering & Management*, *16*(4), 443-456. https://doi.org/10.14743/apem2021.4.412

[15] Vukelic, D., Simunovic, K., Kanovic, Z., Saric, T., Tadic, B., & Simunovic, G. (2021). Multi-objective optimization of steel AISI 1040 dry turning using genetic algorithm. *Neural Computing and Applications*, *33*(19), 12445-12475. https://doi.org/10.1007/s00521-021-05877-z

[16] Ficko, M., Begic-Hajdarevic, D., Hadziabdic, V., & Klancnik, S. (2020). Multi-response optimisation of turning process parameters with GRA and TOPSIS methods. *International Journal of Simulation Modelling*, *19*(4), 547-558. https://doi.org/10.2507/IJSIMM19-4-524

[17] Philip Selvaraj, D., Chandramohan, P., & Mohanraj, M. (2014). Optimization of surface roughness, cutting force and tool wear of nitrogen alloyed duplex stainless steel in a dry turning process using Taguchi method. *Measurement*, *49*, 205-215. https://doi.org/10.1016/j.measurement.2013.11.037

[18] Saric, T., Vukelic, Đ., Simunovic, K., Svalina, I., Tadic, B., Prica, M., & Simunovic, G. (2020). Modelling and prediction of surface roughness in CNC turning process using neural networks. *Tehnicki Vjesnik - Technical Gazette*, *27*(6). https://doi.org/10.17559/TV-20200818114207

[19] Jovicic, G., Milosevic, A., Kanovic, Z., Sokac, M., Simunovic, G., Savkovic, B., & Vukelic, D. (2023). Optimization of dry turning of Inconel 601 alloy based on surface roughness, tool wear, and material removal rate. *Metals*, *13*(6), 1068. https://doi.org/10.3390/met13061068

[20] Vukelic, D., Kanovic, Z., Sokac, M., Santosi, Z., Budak, I., & Tadic, B. (2021). Modelling of micro-turning process based on constant cutting force. *International Journal of Simulation Modelling*, *20*(1), 146-157. https://doi.org/10.2507/IJSIMM20-1-553

[21] Keblouti, O., Boulanouar, L., Azizi, M. W., & Yallese, M. A. (2017). Modeling and multi-objective optimization of surface roughness and productivity in dry turning of AISI 52100 steel using (TiCN-TiN) coating cermet tools. *International Journal of Industrial Engineering Computations*, 71-84. https://doi.org/10.5267/j.ijiec.2016.7.002

[22] Vukelic, D., Simunovic, K., Simunovic, G., Saric, T., Kanovic, Z., Budak, I., & Agarski, B. (2020). Evaluation of an environment-friendly turning process of Inconel 601 in dry conditions. *Journal of Cleaner Production*, *266*, 121919. https://doi.org/10.1016/j.jclepro.2020.121919

[23] Van, A.-L., Nguyen, T.-T., & Dang, X.-B. (2023). Optimization of rough self-propelled rotary turning parameters in terms of total energy consumption and surface roughness. *Tehnicki Vjesnik - Technical Gazette*, *30*(6). https://doi.org/10.17559/TV-20230202000308

[24] Cohen, G., Gilles, P., Segonds, S., Mousseigne, M., & Lagarrigue, P. (2012). Thermal and mechanical modeling during dry turning operations. *The International Journal of Advanced Manufacturing Technology*, *58*(1-4), 133-140. https://doi.org/10.1007/s00170-011-3372-9

[25] Costa, M. I., Rodrigues, D. M., & Leitão, C. (2015). Analysis of AA 6082-T6 welds strength mismatch: Stress versus hardness relationships. *The International Journal of Advanced Manufacturing Technology*, *79*(5-8), 719-727. https://doi.org/10.1007/s00170-015-6866-z

[26] Çavuşoğlu, O., Sürücü, H. İ., Toros, S., & Alkan, M. (2020). Thickness dependent yielding behavior and formability of AA6082-T6 alloy: Experimental observation and modeling.

The International Journal of Advanced Manufacturing Technology, *106*(9-10), 4083-4091. https://doi.org/10.1007/s00170-019-04878-6

[27] Słowiński, P., Grindley, B., Muncie, H., Harris, D., Vine, S., & Wilson, M. (2022). Assessment of cognitive biases in augmented reality: Beyond eye tracking. *Journal of Eye Movement Research*, *15*(3), 4. https://doi.org/10.16910/jemr.15.3.4

[28] Sharma, S., Singh, G., & Singh, D. (2019). Role and performance of different traditional classification and nature-inspired computing techniques in major research areas. *EAI Endorsed Transactions on Scalable Information Systems*, *6*(21), 158419. https://doi.org/10.4108/eai.13-7-2018.158419

[29] Vrigazova, B. (2021). The proportion for splitting data into training and test set for the bootstrap in classification problems. *Business Systems Research Journal*, *12*(1), 228-242. https://doi.org/10.2478/bsrj-2021-0015

[30] Kim, J., Yoon, Y., Park, H.-J., & Kim, Y.-H. (2022). Comparative study of classification algorithms for various DNA microarray data. *Genes*, *13*(3), 494. https://doi.org/10.3390/genes13030494

[31] Soper, D. S. (2021). Greed is good: Rapid hyperparameter optimization and model selection using greedy k-fold cross validation. *Electronics*, *10*(16), 1973. https://doi.org/10.3390/electronics10161973

[32] Chicco, D., Warrens, M. J., & Jurman, G. (2021). The coefficient of determination R-squared is more informative than SMAPE, MAE, MAPE, MSE and RMSE in regression analysis evaluation. *PeerJ Computer Science*, *7*, e623. https://doi.org/10.7717/peerj-cs.623

[33] Origbo, O. A. & Irene, M. I. (2024). Forecasting dead oil viscosity using machine learning processes for Niger delta region. *International Journal of Current Science Research and Review*, *07*(01), 820-830. https://doi.org/10.47191/ijcsrr/V7-i1-81

[34] Garcia, R. F., Feix, E. C., Mendel, H. T., Gonzalez, A. R., & Souza, A. J. (2019). Optimization of cutting parameters for finish turning of 6082-T6 aluminum alloy under dry and RQL conditions. *Journal of the Brazilian Society of Mechanical Sciences and Engineering*, *41*(8), 317. https://doi.org/10.1007/s40430-019-1826-4

[35] Özlü, B. (2021). Sleipner soğuk iş takım çeliğinin tornalanmasında kesme parametrelerinin kesme kuvveti, yüzey pürüzlülüğü ve talaş şekli üzerine etkisinin incelenmesi. *Gazi Üniversitesi Mühendislik Mimarlık Fakültesi Dergisi*, *36*(3), 1241-1252. https://doi.org/10.17341/gazimmfd.668169

[36] Aydin, K. (2023). Investigating cutting force and cutting power when turning AA6082-T4 alloy at cutting depths smaller than tool nose radius. *Kahramanmaraş Sütçü İmam Üniversitesi Mühendislik Bilimleri Dergisi*, *26*(4), 972-982. https://doi.org/10.17780/ksujes.1339021

[37] Astakhov, V. P. & Xiao, X. (2008). A methodology for practical cutting force evaluation based on the energy spent in the cutting system. *Machining Science and Technology*, *12*(3), 325-347. https://doi.org/10.1080/10910340802306017

[38] Nouari, M., List, G., Girot, F., & Coupard, D. (2003). Experimental analysis and optimisation of tool wear in dry machining of aluminium alloys. *Wear*, *255*(7-12), 1359-1368. https://doi.org/10.1016/S0043-1648(03)00105-4

[39] Carrilero, M. S., Bienvenido, R., Sánchez, J. M., Álvarez, M., González, A., & Marcos, M. (2002). A SEM and EDS insight into the BUL and BUE differences in the turning processes of AA2024 Al-Cu alloy. *International Journal of Machine Tools and Manufacture*, *42*(2), 215-220. https://doi.org/10.1016/S0890-6955(01)00112-2

[40] Sreejith, P. S. & Ngoi, B. K. A. (2000). Dry machining: Machining of the future. *Journal of Materials Processing Technology*, *101*(1-3), 287-291. https://doi.org/10.1016/S0924-0136(00)00445-3

[41] Jawahir, I. S., Brinksmeier, E., M'Saoubi, R., Aspinwall, D. K., Outeiro, J. C., Meyer, D., Umbrello, D., & Jayal, A. D. (2011). Surface integrity in material removal processes: Recent advances. *CIRP Annals*, *60*(2), 603-626. https://doi.org/10.1016/j.cirp.2011.05.002

[42] Tougui, I., Jilbab, A., & Mhamdi, J. E. (2021). Impact of the choice of cross-validation techniques on the results of machine learning-based diagnostic applications. *Healthcare Informatics Research*, *27*(3), 189-199. https://doi.org/10.4258/hir.2021.27.3.189

[43] Syed, A. H., Khan, T., Alromema, N. A., Barik, L., AlRababah, A. A. Q., & Aljiffry, M. M. (2022). Covid-19 vaccine dosages and government factors role on the global variation in covid-19 mortality: A statistical and regression analysis. *International Journal of Advanced and Applied Sciences*, *9*(5), 18-31. https://doi.org/10.21833/ijaas.2022.05.003

[44] Ibrahim, T. K., Yawas, D. S., Dan-asabe, B., & Adebisi, A. A. (2023). Taguchi optimization and modelling of stir casting process parameters on the percentage elongation of aluminium, pumice and carbonated coal composite. *Scientific Reports*, *13*, 2915. https://doi.org/10.1038/s41598-023-29839-8

[45] Zhao, Z. (2024). Predicting smartphone prices using machine learning algorithms. *Applied and Computational Engineering*, *95*, 199-209. https://doi.org/10.54254/2755-2721/95/20241765

[46] Amin, A., Rahmawaty, Lautania, M. F., Masrom, S., & Rahman, R. A. (2023). Tree-based machine learning and deep learning in predicting investor intention to public private partnership. *International Journal of Advanced Computer Science and Applications*, *14*(1), 191-195. https://doi.org/10.14569/IJACSA.2023.0140121

[47] Suryaputra Paramita, A. (2022). Implementation of the k-nearest neighbor algorithm for the classification of student thesis subjects. *Journal of Applied Data Sciences*, *3*(3), 128-136. https://doi.org/10.47738/jads.v3i3.66

[48] Ozturk Kiyak, E., Ghasemkhani, B., & Birant, D. (2023). High-level k-nearest neighbors (HLKNN): A supervised machine learning model for classification analysis. *Electronics*, *12*(18), 3828. https://doi.org/10.3390/electronics12183828

[49] Choubey, V., Mishra, S., & K. Pandey, S. (2014). Time series data mining in real time surface runoff forecasting through support vector machine. *International Journal of Computer Applications*, *98*(3), 23-28. https://doi.org/10.5120/17163-7223

[50] Ahmed, S. (2023). A software framework for predicting the maize yield using modified multi-layer perceptron. *Sustainability*, *15*(4), 3017. https://doi.org/10.3390/su15043017

[51] Li, H., Li, W., Pan, X., Huang, J., Gao, T., Hu, L., Li, H., & Lu, Y. (2018). Correlation and redundancy on machine learning performance for chemical databases. *Journal of Chemometrics*, *32*(7), e3023. https://doi.org/10.1002/cem.3023

[52] Gkioulekas, I. & Papageorgiou, L. G. (2019). Piecewise regression analysis through information criteria using mathematical programming. *Expert Systems with Applications*, *121*, 362-372. https://doi.org/10.1016/j.eswa.2018.12.013

[53] Makhfi, S., Dorbane, A., Harrou, F., & Sun, Y. (2024). Prediction of cutting forces in hard turning process using machine learning methods: A case study. *Journal of Materials Engineering and Performance*, *33*, 9095-9111. https://doi.org/10.1007/s11665-023-08555-4

[54] Bagga, P. J., Patel, K. M., Makhesana, M. A., Şirin, Ş., Khanna, N., Królczyk, G. M., Pala, A. D., & Chauhan, K. C. (2023). Machine vision-based gradient-boosted tree and support vector regression for tool life prediction in turning. *The International Journal of Advanced Manufacturing Technology*, *126*, 471-485.

https://doi.org/10.1007/s00170-023-11137-2
[55] Sizemore, N. E., Nogueira, M. L., Greis, N. P., & Davies, M. A. (2020). Application of machine learning to the prediction of surface roughness in diamond machining. *Procedia Manufacturing*, *48*, 1029-1040. https://doi.org/10.1016/j.promfg.2020.05.142
[56] Patel, D., Thakker, H., Kiran, M. B., & Vakharia, V. (2020). Surface roughness prediction of machined components using gray level co-occurrence matrix and bagging tree. *FME Transactions*, *48*(2), 468-475. https://doi.org/10.5937/fme2002468P
[57] Nguyen, V.-H., & Le, T.-T. (2024). Predicting surface roughness in machining aluminum alloys taking into account material properties. *International Journal of Computer Integrated Manufacturing*, *38*(4), 555-576. https://doi.org/10.1080/0951192X.2024.2372252
[58] Gadagi, A., Sivaprakash, B., Adake, C., Deshannavar, U., Hegde, P. G., P., S., Rajamohan, N., & Osman, A. I. (2024). Epoxy composite reinforced with jute/basalt hybrid - Characterisation and performance evaluation using machine learning techniques. *Composites Part C: Open Access*, *14*, 100453. https://doi.org/10.1016/j.jcomc.2024.100453
[59] Prasad, P. K., Dubey, V., & Sharma, A. K. (2022). Surface roughness prediction of AISI 304 steel in nanofluid assisted turning using machine learning technique. *Key Engineering Materials*, *933*, 13-24. https://doi.org/10.4028/p-wwb643
[60] Liang, S., Chen, C., Wu, D., Chen, L., Wu, Q., & Gu, T. T. (2024). An Ensemble Learning Method for the Fault Multi-classification of Smart Meters. *Tehnicki Vjesnik-Technical Gazette*, *31*(5), 1514-1522. https://doi.org/10.17559/tv-20230417000543

Contact information:

Metin ZEYVELİ, Assistant Professor
Karabuk University, Department of Mechatronics Engineering,
Karabuk University Technology Faculty,
Karabuk, Türkiye
E-mail: mzeyveli@karabuk.edu.tr

Murat AYDIN, Assistant Professor
(Corresponding author)
Karabuk University, Department of Industrial Design Engineering,
Karabuk University Technology Faculty,
Karabuk, Türkiye
E-mail: murataydin@karabuk.edu.tr